

# 1. Introduction

Total Knee Arthroplasty (TKA) is a highly effective intervention in ameliorating pain and enhancing the function of a diseased knee (Levine et al. 2016; Gee 2012; "National Joint Registry For England, Wales, Northern Ireland and Isle of Man" 2019; "Australian Orthopaedic Association National Joint Replacement Registry" 2019; "Register of the Orthopaedic Prosthetic Implants" 2017). However, TKA longevity is put at risk due to the wear of the polyethylene (PE) insert ("National Joint Registry For England, Wales, Northern Ireland and Isle of Man" 2019; "Australian Orthopaedic Association National Joint Replacement Registry" 2019; "Register of the Orthopaedic Prosthetic Implants" 2017). The Australian Orthopaedic Association National Joint Replacement Registry (AOANJRR) ("Australian Orthopaedic Association National Joint Replacement Registry" 2019) and the National Joint Registry for England, Wales, Northern Ireland and Isle of Man ("National Joint Registry For England, Wales, Northern Ireland and Isle of Man" 2019) report aseptic loosening to be the primary reason for TKA revision, which is directly caused by PE wear particles (Gallo et al. 2013). Two of the contributing factors to accelerated PE wear are PE type and its manufacturing process (Brown et al. 2017) and increased surface roughness of the metal femoral component (Muratoglu et al. 2004).

For the first factor (PE types), conventional (CPE) and crosslinked polyethylene (XLPE) were studied. Due to the success of XLPEs in total hip replacement, the number of XLPE inserts implanted in knees has increased over the years ("Australian Orthopaedic Association National Joint Replacement Registry" 2019). Though the wear properties of XLPE have been improved, most recent short and mid-term studies except for Stavrakis et al., (Stavrakis et al. 2018) show no clinically significant difference in surface damage (Muratoglu et al. 2003; Willie et al. 2008b), oxidative change (MacDonald et al. 2018), risk or revision (Paxton et al. 2015), radiographic outcomes (Meneghini et al. 2015; Minoda et al. 2009) and average surface deviation or volume change (Liu et al. 2016) between XLPE and CPE inserts. However, in the study by Liu et al., (Liu et al. 2016) samples with different post-irradiation processes were included in the XLPE group, with the majority being remelted samples. Remelted XLPE samples were said to have reduced toughness and resistance to fatigue which could lead to more pitting, abrasion and delamination (Sakellariou et al. 2013), whereas sequentially annealed XLPE inserts were

considered to be more oxidatively stable, preserving crystallinity and mechanical properties of the polyethylene (Medel et al. 2007). These differences could have affected the results seen within the XLPE group. Therefore, for the current study only annealed XLPE and CPE inserts were analysed and compared.

For the second factor (surface roughness), several laboratory tests have shown the association between wear of PE and surface roughness of the femoral component (DesJardins, Burnikel, and LaBerge 2008; Jaber et al. 2015; Affatato, Bracco, and Sudanese 2013; Ruggiero, Merola, and Affatato 2017; Affatato, Merola, and Ruggiero 2019; Saikko, Vuorinen, and Revitzer 2016). While *in vitro* tests give results under standardized test conditions, they do not mimic human body conditions. An increased femoral component roughness was observed in many retrieval studies, with an average time *in vivo* of  $72 \pm 54$  months (Scholes et al. 2013; Kennard et al. 2017; Heyse et al. 2014). However, there are very few *ex vivo* studies that have correlated this femoral roughness change to the damage of the corresponding PE inserts. Scholes et al., investigated retrieved TKAs, and found no correlation between the increased femoral component roughness and a semi-quantitative scoring value obtained for PE surface damage (Scholes et al. 2013). In contrast, Alvarez et al., found a linear trend for surface roughness of the retrieved unicondylar femoral component and PE damage area value (calculated as the percentage of different damage modes covering the total articular surface) (Alvarez 2012). The authors looked at non-conforming fixed unicondylar inserts which showed evident creep (which the authors termed deformation) due to non-conformity. Given, the contrasting and limited information, the current study aimed to better understand the relationship between femoral roughness and PE damage *ex vivo* in the two modern retrieved designs.

We performed a matched-pair analysis of retrieved TKA components. Damage scoring, 3D laser scanning and 3D surface profilometry were used to analyze two different TKA designs. The aims of the current study were to investigate if there was any difference in the damage score or deviation values between the two PE insert types and to assess if there was any correlation between the femoral roughness and deviation of the PE in both TKA designs.

## 2. Materials and Methods

### 2.1 Retrieval process

Approval was obtained from the appropriate Research Ethics Committee (09/H0906/72) prior to the retrieval analysis. Two specific designs, DePuy Sigma (n =40) (DePuy Inc, Warsaw, IN, USA) and Stryker Triathlon (n =14) (Stryker Crop, Kalamazoo, MI, USA) were selected for the current study. Nine retrieved Sigma were matched with nine Triathlon components from the larger cohort for insert type (Cruciate retaining design, CR), bearing type (fixed bearing), cemented fixation, time *in vivo* and age at revision. The patient and implant variables are given in Table 1.

Explant Characteristics	Sigma (n=9)	Triathlon (n=9)	p-value
Time <i>in vivo</i> (months, m)	27 ± 10 (range, 13-36)	36 ± 23 (range, 13-79)	0.23
Age at revision (years, y)	62 ± 9 (range, 42-72)	68 ± 12 (range, 53-85)	0.34
Sex	Male - 6 Female - 3	Male - 5 Female - 4	N/A
Side	Left - 6 Right - 3	Left - 4 Right - 5	N/A
Reasons for revision	Pain/Stiffness - 3 Instability - 4 Malalignment - 2	Pain/Stiffness - 6 Infection - 3	N/A
Femoral component size - PE insert size (number of explants in the combination)	4 - 3 (4), 3 - 3 (1), 2.5 - 3 (1), 5 - 4 (2)	5 - 4 (4), 4 - 4 (2), 5 - 5 (3)	N/A

**Table 1:** Patient and implant variables of the eighteen retrieved total knee components (mean ± standard deviation)

The femoral components of both designs were made of Cobalt-chromium (CoCr) alloy. The tibial PE insert of the Sigma cohort was fabricated from compression-molded GUR 1020, sterilized with gamma irradiation and packaged in vacuum foil (CPE). In contrast, the PE insert of the Triathlon cohort was compression-molded GUR 1020 that is sequentially irradiated and annealed three times for a total dose of 90 kGy and then sterilized in gas plasma (XLPE) (Sisko et al. 2017) (figure 1). CPE remains the gold standard for many tibial inserts, however XLPE is known to have better wear and oxidative properties (Muratoglu et al. 2004) (Huot et al. 2010). It

should be noted that size 4, 5 femoral component and size 4 PE insert were not the same for Sigma and Triathlon cohorts (table 1). Reference (pristine) PE inserts of size 3, 4 for Sigma cohort and size 4, 5 for Triathlon cohort were obtained. A brand-new femoral component (reference) for the both cohorts were also obtained.

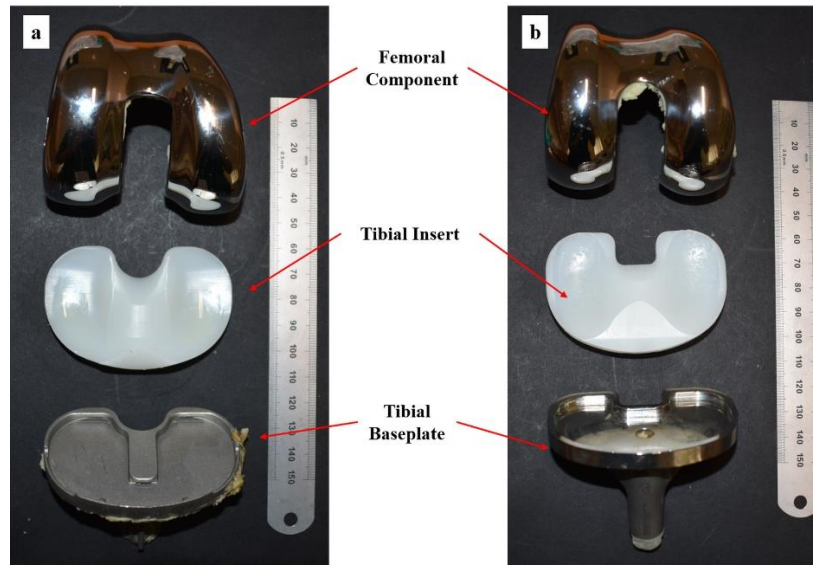


**Figure 1:** (a) Stryker Triathlon (Femoral component – Cobalt-Chromium (CoCr) alloy, Tibial Insert – XLPE, Tibial baseplate – non-polished CoCr); (b) DePuy Sigma (Femoral component – CoCr alloy, Tibial Insert – CPE, tibial baseplate – polished CoCr)

## **2.2 Radiographic analysis**

The pre-revision radiographs of the studied patients were obtained to measure the posterior tibial slope angle (PTSA), medial proximal tibial angle (MPTA) and tibiofemoral angle (TFA).

Radiographs were not available for 1 of the 9 patients for each of the cohorts.

PTSA was determined on a lateral view radiograph where a longitudinal axis (vertical line) is drawn along the center of the tibial shaft and a horizontal axis (perpendicular line) is drawn along the edges of the tibial implant. The resulting angle from the intersecting lines was subtracted from  $90^\circ$  which represented the slope angle (figure 2a) (Dejour and Bonnin 1994).

MPTA was determined on an anterior-posterior view radiograph by measuring the medial angle formed between the knee joint line of the tibia and a line passing through the center of the tibial medullary canal (figure 2b) (Bach et al. 2001). Tibiofemoral angle (TFA) was defined as the

angle between the femoral anatomical axis and the tibial anatomical axis (Petersen and Engh 1988). Anatomical axes of the femur and tibia were defined as a line drawn through two mid points of the bone at a distance of 100 mm and 150 mm from the knee joint line (Sheehy et al. 2011). To assess the alignment, TFA value was subtracted from 180°; a negative value corresponded to a varus alignment and a positive value corresponded to a valgus alignment (figure 2c).

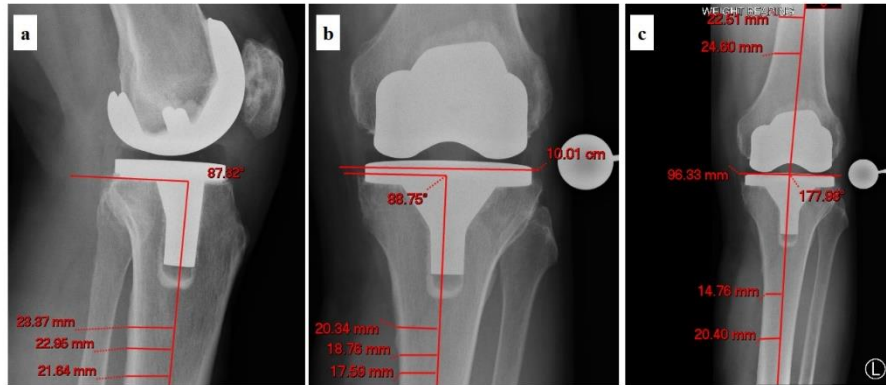


**Figure 2:** Measurement made on a DePuy component (a) PTSA (b) MPTA (c) TFA

### ***2.3 Visual assessment and scoring of PE insert***

The articular surfaces of the all the retrieved PE inserts were assessed using a non-contact vision measuring system (Mitutoyo Quick Scope) at 25x magnification (50x lens and 0.5x zoom). The surface was divided into ten regions; 0-3 regions represented the medial plateau, 4-7 represented the lateral plateau and 8,9 the non-bearing surface (figure 3).

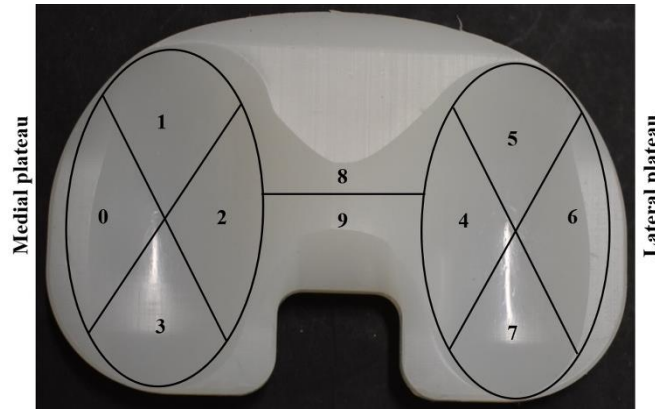


**Figure 3:** The articular surface of the PE insert was divided into 10 different regions for damage mode assessment

Each region was scored for seven different damage modes, adopting the method of Brandt et al (Brandt et al. 2012). The seven damage modes were creep (surface deformation), pitting, embedded debris, scratching, burnishing, abrasion and delamination. Each damage mode was scored based on severity of damage (SS, severity score) and percentage area that the damage has affected (AS, area score). An AS of 0,1,2,3...10 was assigned to each damage mode which corresponded to a damage area of 0%, 0-10%, 10-20%, 20-30%.... 90-100%. In terms of SS, 0 represented no damage, 0.33 represented mild damage, 0.66, medium damage and 1, adverse damage. The product of AS and SS gave the score of each region and the summation of all these scores gave the overall component damage score. The maximum component damage score for each PE insert would be 700 (maximum score of 10 for all seven damage modes for ten different regions).

#### **2.4 Surface deviation analysis of the tibial components**

The articular surfaces of all inserts were scanned using a 3D laser scanner (NextEngine, Santa Monica, CA). Five individual scans were taken for all the retrieved inserts and size-matched pristine inserts at a 0° inclination at every 30° revolution. The undesirable (not the focus of study) areas in the scans were removed and the five scans were aligned using three reference points in the manufacturer's software (NextEngine, ScanStudio, Ver 2.0.2). The final combined model was a point cloud of ~250,000 points with a resolution of 63 micron (Stoner et al. 2013). The xyz point cloud was converted into a mesh before exporting for further analysis. Processed

3D models were imported into GOM inspect software (Hotfix 2, Rev. 113294, GOM Inspect 2018). The retrieved sample was aligned to the size-matched pristine model using an initial alignment tool first and then a best-fit alignment tool (which uses a least-squares algorithm, where the sum of squared distance between two scans are minimized and the scans are realigned). After alignment, surface comparison between the two was made.

The average deviation (distance between the closest point pairs of the retrieved and pristine sample) was calculated (Liu et al. 2016; Kurdziel et al. 2018). The term ‘deviation’ defines dimensional changes between the surfaces due to wear and creep, as it is difficult to differentiate between these two phenomena (Stoner et al. 2013). The regions of interest for the current study were the medial and the lateral plateaus (figure 2). The deviations of these regions were calculated.

## **2.5 Surface profilometry of the femoral components**

Surface roughness measurements on the retrieved and pristine femoral components of the Sigma and Triathlon cohorts were obtained using a non-contacting white light interferometric profilometer (Newview 5000, Zygo, Middlefield, CT, USA) as used in previous explant studies (Scholes et al. 2013; Holleyman et al. 2015; Joyce et al. 2009). The measurements were obtained at 20x magnification (2x zoom and 10x lens) providing an area of view of 317x238  $\mu\text{m}$ . The vertical resolution of the optical surface profilometer is less than 1nm. Before the analysis all the explants were cleaned using isopropanol.

Only one roughness parameter  $S_q$  (root-mean square of the deviation in the peaks and valleys from the mean line of the sampling area) was chosen to assess its correlation to the corresponding PE deviation value. Most studies report  $S_a$  (mean of the deviations in peaks and valleys from the mean line of the sampling area) when analyzing the changes in roughness of the surface but in the current work  $S_q$  was chosen because it is more sensitive to large deviations from the mean line (Gadelmawla et al. 2002; "BS EN ISO 4287 - 1998+A1-2009. Geometric product specification (GPS) surface texture profile method terms, definitions and surface texture parameters." 2009) than  $S_a$ . Fifteen roughness measurements were made at two different flexion angles of approximately 30° and 60° so a total of thirty points were taken on each femoral

condyle giving an aggregate of sixty points for each sample (figure 4). This matched the method followed in a previous study (Chacko Rajan et al. 2019).

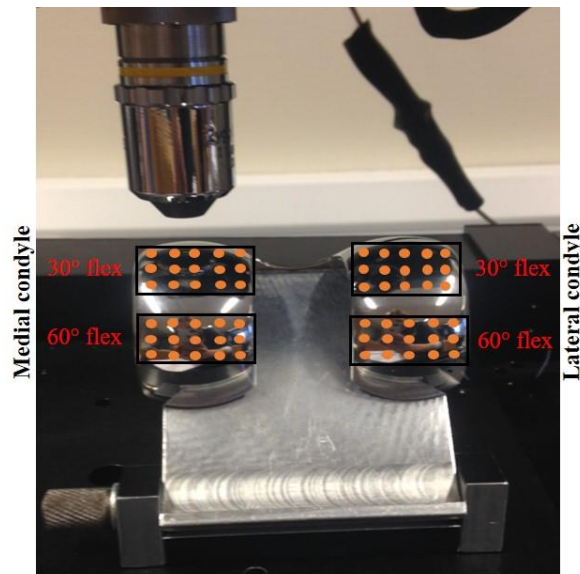


**Figure 4:** Representation of 60 roughness measurements made at two different flexion angles on the femoral component with 30 measurements carried out on each condyle

## **2.6 Statistical analysis**

The data collected was analysed using IBM SPSS version 25 (SPSS Inc., Chicago, IL, USA). Throughout the current study, the mean values were calculated for all parameters along with standard deviation (SD). Based on the distribution of retrieval data (assessed using histogram and Kolmogorov Smirnov test) either t-test (parametric) or Mann-Whitney (non-parametric) tests were carried out to compare the difference in the deviation and damage score between Sigma and Triathlon cohort. Also, the difference in roughness values between reference and retrieved femoral component for both cohorts. Sixty roughness measurements were obtained for each reference and retrieved femoral component. A total of  $60 \times 9 = 540$  values was measured for each retrieved cohort. Correlation between deviations and roughness values were assessed using linear regression analysis. The level of statistical significance was considered at  $p < 0.05$ .

### 3. Results

#### 3.1 Radiographic analysis

No significant difference in tibial slope angle (PTSA), proximal tibial angle (MPTA) and tibiofemoral angle (TFA) were found between the Sigma and Triathlon cohorts (table 2). There was no correlation between the time *in vivo* and tibial slope angles or age at revision and tibial slope angles; a similar pattern of correlation was also seen with the tibiofemoral angle for the Sigma and Triathlon cohorts (results not presented).

Angle measured	DePuy Sigma mean $\pm$ standard deviation (range)	Stryker Triathlon mean $\pm$ standard deviation (range)	p-value
PTSA	7.32° $\pm$ 6.14° (1.06°-21.03°)	4.57° $\pm$ 2.86° (1.51°-10.55°)	0.38
MPTA	86.69° $\pm$ 2.93° (82.25° $\pm$ 91.08°)	87.84° $\pm$ 3.92° (79.89°-91.86°)	0.51
TFA	173.01° $\pm$ 2.72° (170.01°-176.92°)	173.59 $\pm$ 3.55° (167.22°-177.65°)	0.71

**Table 2:** Slope angle and tibiofemoral angle of retrieved Sigma and Triathlon cohort

#### 3.2 Visual assessment and scoring of PE insert

The average damage score observed for the Sigma (CPE) cohort (38.52  $\pm$  24.28) was not statistically significantly different to the Triathlon (XLPE) cohort (38.55  $\pm$  20.80) ( $p = 0.98$ ). Burnishing was the most common damage mode observed on all the PE samples. No delamination was observed. Embedded debris was only found in one Sigma (CPE) sample. Two samples in the Sigma cohort were observed to have substantial damage in comparison to all the other samples. The average score of the different damage modes for bearing surface, non-bearing surface and total surface for Sigma (CPE) and Triathlon (XLPE) cohorts are given in table 3. Average scores for the bearing surface were similar for both the cohorts with burnishing and pitting being the two predominant damage modes in the Sigma (CPE) and burnishing and scratching in the Triathlon (XLPE) cohort. There was more creep found in the bearing surface of Sigma (CPE) than Triathlon (XLPE) cohort (Table 3). Perhaps surprisingly, the non-bearing

surface also showed damage modes with mild scratching seen in the Sigma (CPE) and burnishing, pitting and deformation seen in the Triathlon (XLPE) cohort. No correlation was found between damage score and time *in vivo* or damage score and age at revision for either of the cohorts (results not presented).

Damage mode	Bearing surface (score)			Non-bearing surface (score)			Total		
	Sigma	Triathlon	<i>P</i> value	Sigma	Triathlon	<i>P</i> value	Sigma	Triathlon	<i>P</i> value
<b>Burnishing</b>	20.47 ± 14.76	22.46 ± 10.12	0.55	0.00 ± 0.00	0.26 ± 0.28	0.05	20.47 ± 14.76	22.72 ± 10.25	0.71
<b>Pitting</b>	10.24 ± 15.99	6.93 ± 4.85	0.22	0.00 ± 0.00	0.11 ± 0.23	0.44	10.24 ± 15.99	7.04 ± 4.99	0.22
<b>Scratching</b>	6.28 ± 8.14	8.42 ± 9.68	0.60	0.15 ± 0.34	0.00 ± 0.00	0.44	6.42 ± 8.09	8.42 ± 9.68	0.66
<b>Abrasion</b>	0.80 ± 2.42	0.22 ± 0.66	1.00	0.00 ± 0.00	0.00 ± 0.00	1.00	0.81 ± 2.42	0.22 ± 0.66	1.00
<b>Creep (surface deformation)</b>	0.55 ± 0.37	0.11 ± 0.23	0.01	0.00 ± 0.00	0.03 ± 0.11	0.73	0.55 ± 0.37	0.15 ± 0.29	0.04
<b>Embedded debris</b>	0.03 ± 0.11	0.00 ± 0.00	0.73	0.00 ± 0.00	0.00 ± 0.00	1.00	0.04 ± 0.11	0.00 ± 0.00	0.73
<b>Delamination</b>	0.00 ± 0.00	0.00 ± 0.00	1.00	0.00 ± 0.00	0.00 ± 0.00	1.00	0.00 ± 0.00	0.00 ± 0.00	1.00
<b>Total</b>	38.38 ± 24.23	38.14 ± 20.39	0.98	0.15 ± 0.34	0.48 ± 0.57	0.16	38.52 ± 24.28	38.55 ± 20.80	0.99

**Table 3:** Damage score (mean ± standard deviation) of seven different damage modes on the articular surface of Sigma (CPE) and Triathlon (XLPE) inserts

### **3.3 Surface deviation analysis of the tibial components**

Different surface deviation patterns were observed in the Sigma and Triathlon cohorts. In the Sigma cohort, a pattern was seen where deviation covered most of medial and lateral plateau surface (figure 5a); a separate combination pattern was also seen where the deviation focused on the center and on the posterior or anterior edges of the plateau (figure 5b). For the Triathlon cohort, an asymmetric pattern was observed where the deviation was asymmetrically (center, outer and inner edge) distributed across the medial and lateral plateau (figure 5c); separately, a symmetric pattern was also seen where the deviation was symmetrically distributed across the outer edges of the plateaus (figure 5d). The average medial plateau deviation was  $-0.13 \pm 0.11$  mm for the Sigma (CPE) cohort and  $-0.10 \pm 0.04$  mm for the Triathlon cohort (XLPE). The average lateral plateau deviation was  $-0.11 \pm 0.11$  mm for the Sigma (CPE) cohort and  $-0.11 \pm$

0.04 mm for the Triathlon cohort (XLPE). No significant difference was observed between the medial or lateral plateau deviation of Sigma (CPE) and Triathlon (XLPE) (medial deviation,  $p = 0.45$ ; lateral deviation,  $p = 0.96$ ).

No correlation was found between deviation and time *in vivo* or deviation and age at revision for both the cohorts (results not presented).

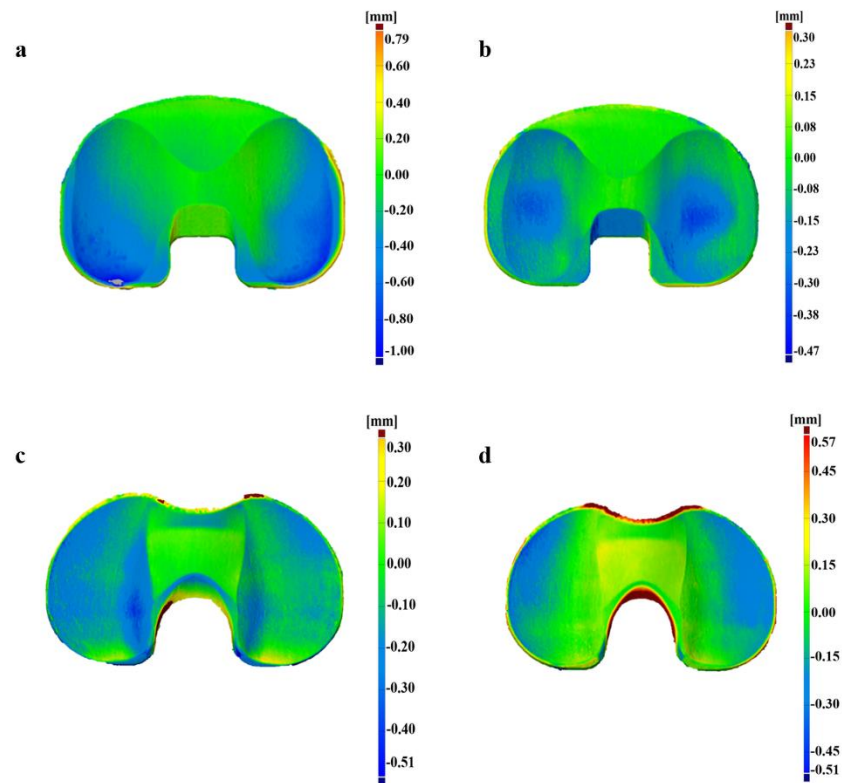
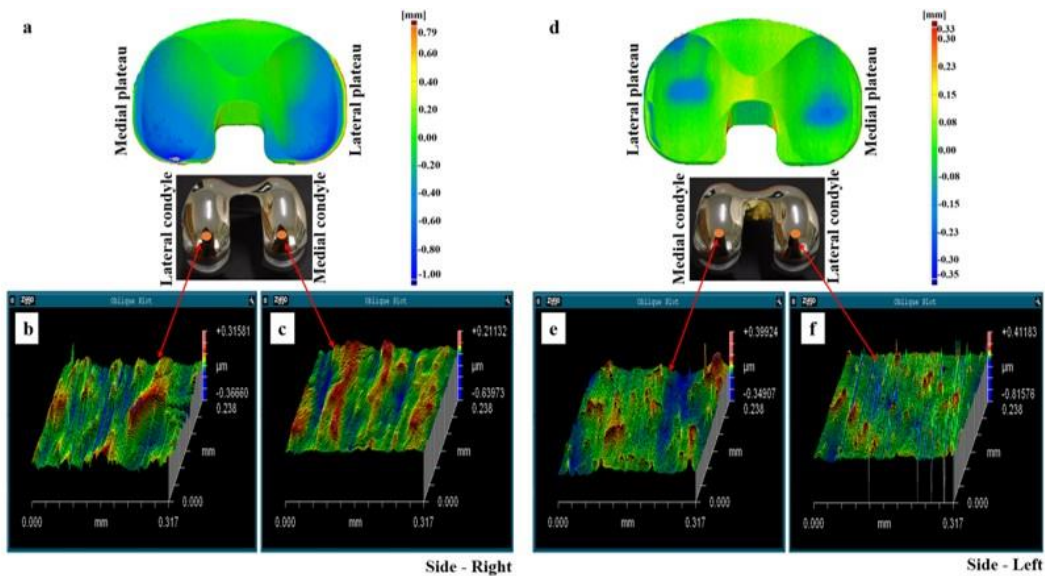


**Figure 5:** Two deviation patterns were found for the Sigma cohort (a) Entire surface (b) Combination. Two different patterns were seen for the Triathlon cohort (c) Asymmetric (d) Symmetric. Blue area indicates deviation below the original surface, green area indicates no deviation and yellow/red area indicates deviation above the original surface

### 3.4 Correlation between femoral component roughness and tibial deviation

The average  $S_q$  values of the medial and lateral condyles of the retrieved Sigma components were  $0.054 \pm 0.040\mu\text{m}$  and  $0.052 \pm 0.034\mu\text{m}$ , respectively. The average  $S_q$  values of the medial and lateral condyle of the reference Sigma femoral component were  $0.044 \pm 0.006\mu\text{m}$  and  $0.034 \pm 0.06\mu\text{m}$ , respectively. Similarly, the  $S_q$  value of the medial and lateral condyle of the retrieved Triathlon components were  $0.069 \pm 0.206\mu\text{m}$  and  $0.082 \pm 0.183\mu\text{m}$ , respectively, while these values for the reference Triathlon femoral component were  $0.032 \pm 0.007\mu\text{m}$  and  $0.034 \pm 0.009\mu\text{m}$ , respectively.

Only the average  $S_q$  value of the lateral condyle of the retrieved Sigma cohort showed a significant difference ( $p < 0.001$ ) in comparison to its reference value.



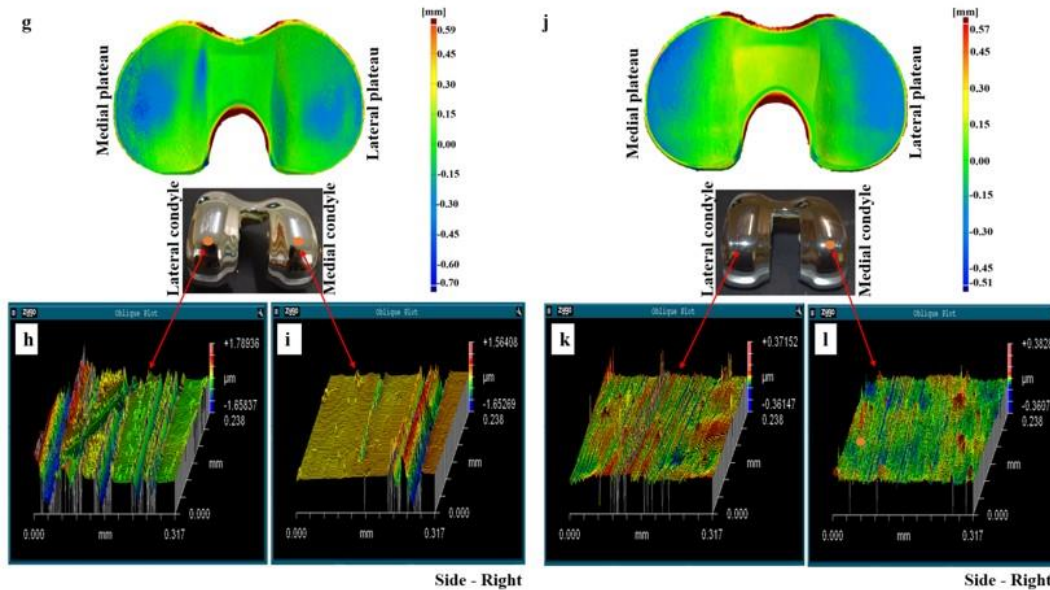


**Figure 6:** Surface deviation maps of DePuy Sigma PE (a) S1 (Entire surface pattern) (d) S6 (combination pattern), Stryker Triathlon XLPE (g) T2 (asymmetric pattern) (j) T5 (symmetric pattern); surface topography images of femoral component, DePuy Sigma (b) region on lateral condyle of S1 (c) region on medial condyle of S1 (e) region of medial condyle of S6 (f) region on lateral condyle of S6, Stryker Triathlon (h) region on the lateral condyle of T2 (i) region on the medial condyle of T2 (k) region on the lateral condyle of T5 (l) region on the medial condyle of T5

The 3D surface profile of a region on the medial (figure 6 (c, e, i, l)) and lateral condyle (figure 6 (b, f, h, k)) of four samples, two from each cohort (DePuy Sigma CPE: S1, S6 and Stryker Triathlon XLPE: T2, T5 ), is given in figure 6. A positive correlation was found between the lateral plateau deviation and the lateral femoral condyle roughness of the Sigma cohort (figure 7a). However, the medial side did not show such a correlation (figure 7a). The medial and lateral side of the Triathlon cohort did not show any correlation (figure 7b). An overall regression analysis of the medial and lateral side of both the cohorts also showed no correlation (results not presented).

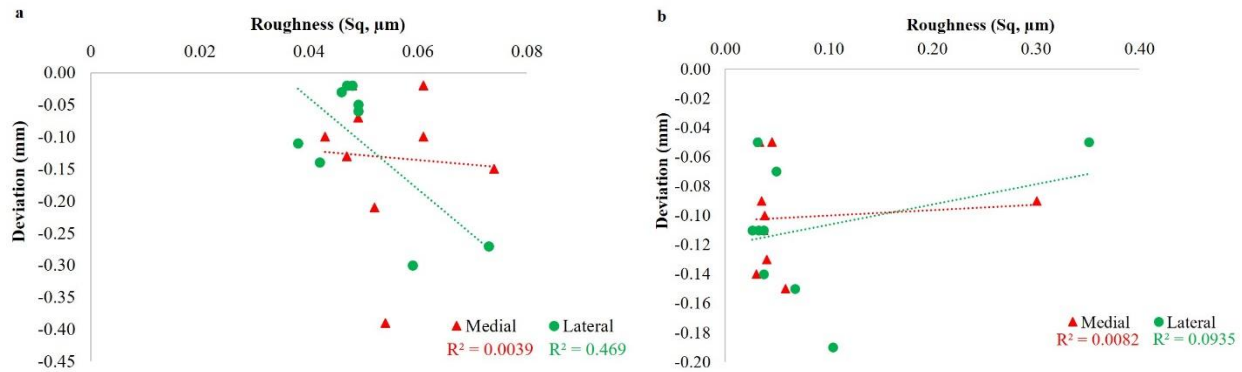


**Figure 7:** Correlation between femoral roughness and PE deviation of medial and lateral side of (a) DePuy Sigma (b) Stryker Triathlon

## 4. Discussion

The difference in damage and deviation between the CPE and XLPE cohorts in TKA were analysed in order to add to the limited literature available on this topic. Also, an *ex vivo* correlation study between femoral roughness and deviation of PE was carried out which, to our knowledge, has not been reported previously.

Concerning the different types of polyethylene, burnishing, pitting and scratching were observed to be the primary modes of damage in the Sigma (CPE) and Triathlon (XLPE) cohorts.

Burnishing was the most common damage mode in both cohorts, this has also been observed in previous studies (Stavrakis et al. 2018). The scratching damage seen in the non-bearing region of the Sigma (CPE) cohort could be due to two samples that were retrieved due to malalignment, which could have led to this damage. The damage was not from explantation but rather occurred *in vivo*. There are previous studies that reported scratching in the non-bearing region of the PE insert (Willie et al. 2008b; Liu et al. 2016). For the Triathlon (XLPE) cohort, the tibial insert had a less-conforming rotatory-arc design which facilitates internal and external rotation (Stoddard et al. 2013), and this could have led to damage on the non-bearing surface, seen in most of the samples. There was less creep seen in the bearing surface of Triathlon (XLPE) than Sigma (CPE) cohort. There are two possible reasons for this. First, XLPE has better creep resistance than CPE. A clinical study of hips by Sato et al., 2012 stated that the creep of XLPE

was 0.19 mm compared to 0.44 mm for CPE (Sato et al. 2012). Second, it could be due to the reasons of revision. In the Sigma (CPE) cohort most of the samples revised for instability showed creep. In these cases, there is a high chance of the femoral component to move off its normal tracking path causing high contact stress in one particular area which leads to deformation.

The two different deviation patterns observed in the Sigma (CPE) and Triathlon (XLPE) cohorts could be caused by designs. For example, the Sigma PE inserts have a higher tibiofemoral conformity which leads to greater contact area, thus there was more centrally focused deviation was observed. In contrast, the PE insert design in the Triathlon cohort was a rotary arc design which showed deviation in the outer, inner edges and at the center. It could also be due to size mismatch between femoral component and the tibial insert, for example when a femoral component of size 5 is matched with a tibial insert of size 4 or vice versa. In the current study, we see this type of mismatch in seven samples of Sigma and four samples of Triathlon cohort (table 1). The deviation pattern observed in the current study was not limited to the traditional posterior sliding of the lateral femoral condyle on the lateral plateau and pivoting movement of the medial femoral condyle on the medial plateau (Dennis et al. 2003). Similar deviation pattern to the current study has also been observed in previous studies (Stoner et al. 2013; Anderson 2017). The surface deviation values on the medial plateau and the lateral plateau were not statistically significantly different between the two cohorts. There was no significant difference observed in the medial and lateral deviation values within the same design for both the cohorts (Sigma,  $p = 0.19$ ; Triathlon,  $p = 0.50$ ). This lack of difference could be due to the short time *in vivo* ( $32 \pm 18$  months). The finding of the current study corroborates other previous studies (Meneghini et al. 2015; Willie et al. 2008a; Hinarejos et al. 2013) which also found no significant difference between CPE ( $53 \pm 13$  months) and XLPE ( $32 \pm 26$  months) inserts after a short time *in vivo*.

The only correlation seen *ex vivo* was between the lateral femoral condyle roughness and the lateral plateau deviation of the Sigma cohort. This correlation could be due to the significant difference observed in the roughness of the retrieved lateral femoral condyle in comparison to the reference lateral femoral condyle. Alternatively, this correlation could be explained by the two Sigma PE samples that were observed to have notable damage (figure 7a). The high standard

deviation seen in the roughness of the Triathlon cohort was due to two samples which showed a substantial anterior-posterior damage pattern.

There are several limitations to the current study. Since the current work is the analysis of failed prostheses, they might not truly represent well-functioning TKAs. Only a small sample size with short time *in vivo* was analysed, however these are modern designs and so the numbers available at our center were limited. Having two different femoral designs might mask any difference in the surface deviation or damage score between the CPE and XLPE inserts. However, several studies have found that there was no distinction in the performance of two different femoral designs (Luo et al. 2019; Lee et al. 2018; Hinarejos et al. 2016; Kim et al. 2015; Sharma 2018). For the deviation analysis, the original dimensions of the tibial PE inserts were unknown, however we compared the samples with pristine inserts of the same design from the same manufacturer. With the 3D laser scanning technique, it was hard to differentiate between wear and creep, whereas with the damage scoring method, a specific score for creep and other surface damage modes could be obtained.

## **5. Conclusion**

This is the first *ex vivo* study to correlate femoral roughness with the surface deviation of PE inserts. There was no major difference in the damage score or deviation between the Sigma (CPE) and Triathlon (XLPE) cohorts. No correlation was found between the roughness of femoral components and deviation of PE inserts except on the lateral side of the Sigma cohort. Retrieval studies help to give important insights into the performance of implants in the human body.

## References

- Affatato, Saverio, Pierangiola Bracco, and Alessandra Sudanese. 2013. 'In vitro wear assessments of fixed and mobile UHMWPE total knee replacement', *Materials & Design*, 48: 44-51.
- Affatato, Saverio, Massimiliano Merola, and Alessandro Ruggiero. 2019. 'Tribological performances of total knee prostheses: Roughness measurements on medial and lateral compartments of retrieved femoral components', *Measurement*, 135: 341-47.
- Alvarez, E et al. 2012. "Relationship between Surface Roughness and Articular Wear for Cobalt-Chrome on Polyethylene Bearing Couples: Evaluation of Retrieved Unicondylar Knee Replacements." In *ORS Annual Meeting*.
- Anderson, F.L; Koch, C.N; Elpers, M.E; Wright, T.M; Haas, S.B; Heyse, T.J. 2017. 'Oxidised Zirconium versus cobalt alloy bearing surfaces in total knee arthroplasty ', *The Bone & Joint Journal*, 99: 793 - 800.
- "Australian Orthopaedic Association National Joint Replacement Registry." In. 2019. *20th Annual Report*.
- Bach, C.M., I.E. Steingruber, S. Peer, M. Nogler, C. Wimmer, and M. Ogon. 2001. 'Radiographic Assesment in Total Knee Arthroplasty', *Clinical orthopaedics and related research*, 385: 144-50.
- Brandt, J. M., C. M. Haydon, E. P. Harvey, R. W. McCalden, and J. B. Medley. 2012. 'Semi-quantitative assessment methods for backside polyethylene damage in modular total knee replacements', *Tribology International*, 49: 96-102.
- Brown, T.S, D. W. Van Citters, D. J. Berry, and M. P. Abdel. 2017. 'The use of highly crosslinked polyethylene in total knee arthroplasty', *The Bone & Joint Journal*: 996-1002.
- "BS EN ISO 4287 - 1998+A1-2009. Geometric product specification (GPS) surface texture profile method terms, definitions and surface texture parameters." In. 2009.
- Chacko Rajan, S., O. Bretcanu, D. J. Weir, D. J. Deehan, and T. J. Joyce. 2019. 'First tribological assessment of retrieved Oxinium patellofemoral prostheses', *J Mech Behav Biomed Mater*, 90: 665-72.
- Dejour, D. H., and M. Bonnin. 1994. 'Tibial translation after anterior cruciate ligament rupture', *The Journal of bone and joint surgery. British volume*: 745-49.
- Dennis, D. A., R. D. Komistek, M. R. Mahfouz, B. D. Haas, and J. B. Stiehl. 2003. 'Multicenter determination of in vivo kinematics after total knee arthroplasty', *Clin Orthop Relat Res*: 37-57.
- DesJardins, John D., Brian Burnikel, and Martine LaBerge. 2008. 'UHMWPE wear against roughened oxidized zirconium and CoCr femoral knee components during force-controlled simulation', *Wear*, 264: 245-56.
- Gadelmawla, ES, MM Koura, TMA Maksoud, IM Elewa, and HH Soliman. 2002. 'Roughness parameters', *Journal of Materials Processing Technology*, 123: 133-45.
- Gallo, Jiri, Stuart B. Goodman, Yrjö T. Kontinen, Markus A. Wimmer, and Martin Holinka. 2013. 'Osteolysis around total knee arthroplasty: a review of pathogenetic mechanisms', *Acta biomaterialia*, 9: 8046-58.

- Gee, A.O; Lee, G-C;. 2012. 'Alternative bearings in Total Knee Arthroplasty', *The American Journal of Orthopedics*, 41: 280-83.
- Heyse, T. J., M. E. Elpers, D. H. Nawabi, T. M. Wright, and S. B. Haas. 2014. 'Oxidized zirconium versus cobalt-chromium in TKA: profilometry of retrieved femoral components', *Clin Orthop Relat Res*, 472: 277-83.
- Hinarejos, P., I. Pinol, A. Torres, E. Prats, G. Gil-Gomez, and L. Puig-Verdie. 2013. 'Highly crosslinked polyethylene does not reduce the wear in total knee arthroplasty: in vivo study of particles in synovial fluid', *J Arthroplasty*, 28: 1333-7.
- Hinarejos, P., L. Puig-Verdie, J. Leal, X. Pelfort, R. Torres-Claramunt, J. Sanchez-Soler, and J. C. Monllau. 2016. 'No differences in functional results and quality of life after single-radius or multiradius TKA', *Knee Surg Sports Traumatol Arthrosc*, 24: 2634-40.
- Holleyman, Richard J, Susan C Scholes, David Weir, Simon S Jameson, Jim Holland, Tom J Joyce, and David J Deehan. 2015. 'Changes in surface topography at the TKA backside articulation following in vivo service: a retrieval analysis', *Knee Surgery, Sports Traumatology, Arthroscopy*, 23: 3523-31.
- Huot, J. C., D. W. Van Citters, J. H. Currier, B. H. Currier, M. B. Mayor, and J. P. Collier. 2010. 'Evaluating the suitability of highly cross-linked and remelted materials for use in posterior stabilized knees', *J Biomed Mater Res B Appl Biomater*, 95: 298-307.
- Jaber, S. A., A. Ruggiero, S. Battaglia, and S. Affatato. 2015. 'On the roughness measurement on knee prostheses', *Int J Artif Organs*, 38: 39-44.
- Joyce, T. J., D. J. Langton, S. S. Jameson, and A. V. F. Nargol. 2009. 'Tribological analysis of failed resurfacing hip prostheses and comparison with clinical data', *Proceedings of the Institution of Mechanical Engineers, Part J: Journal of Engineering Tribology*, 223: 317-23.
- Kennard, Emma, Susan C Scholes, Raghavendra Sidaginamale, Rajkumar Gangadharan, David J Weir, James Holland, David Deehan, and Thomas J Joyce. 2017. 'A comparative surface topographical analysis of explanted total knee replacement prostheses: Oxidised zirconium vs cobalt chromium femoral components', *Medical Engineering and Physics*, 50: 59-64.
- Kim, D. H., D. K. Kim, S. H. Lee, K. I. Kim, and D. K. Bae. 2015. 'Is Single-Radius Design Better for Quadriceps Recovery in Total Knee Arthroplasty?', *Knee Surg Relat Res*, 27: 240-6.
- Kurdziel, M. D., M. D. Newton, S. Hartner, K. C. Baker, and J. M. Wiater. 2018. 'Quantitative evaluation of retrieved reverse total shoulder arthroplasty liner surface deviation and volumetric wear', *J Orthop Res*.
- Lee, M., J. Y. Chen, H. Ying, P. H. Nee, D. K. J. Tay, P. L. Chin, C. S. Lu, L. N. Nung, and Y. S. Jin. 2018. 'Quality of life and functional outcome after single-radius and multi-radius total knee arthroplasty', *J Orthop Surg (Hong Kong)*, 26: 2309499018792417.
- Levine, R. A., K. A. Lewicki, J. H. Currier, M. B. Mayor, and D. W. Van Citters. 2016. 'Contribution of micro-motion to backside wear in a fixed bearing total knee arthroplasty', *J Orthop Res*, 34: 1933-40.
- Liu, T., C. Esposito, M. Elpers, and T. Wright. 2016. 'Surface Damage Is Not Reduced With Highly Crosslinked Polyethylene Tibial Inserts at Short-term', *Clin Orthop Relat Res*, 474: 107-16.

- Luo, Z., Z. Luo, H. Wang, Q. Xiao, F. Pei, and Z. Zhou. 2019. 'Long-term results of total knee arthroplasty with single-radius versus multi-radius posterior-stabilized prostheses', *J Orthop Surg Res*, 14: 139.
- MacDonald, D. W., G. B. Higgs, A. F. Chen, A. L. Malkani, M. A. Mont, and S. M. Kurtz. 2018. 'Oxidation, Damage Mechanisms, and Reasons for Revision of Sequentially Annealed Highly Crosslinked Polyethylene in Total Knee Arthroplasty', *J Arthroplasty*, 33: 1235-41.
- Medel, F. J., P. Pena, J. Cegonino, E. Gomez-Barrena, and J. A. Puertolas. 2007. 'Comparative fatigue behavior and toughness of remelted and annealed highly crosslinked polyethylenes', *J Biomed Mater Res B Appl Biomater*, 83: 380-90.
- Meneghini, R. M., L. R. Lovro, S. A. Smits, and P. H. Ireland. 2015. 'Highly Cross-Linked Versus Conventional Polyethylene in Posterior-Stabilized Total Knee Arthroplasty at a Mean 5-Year Follow-up', *J Arthroplasty*, 30: 1736-9.
- Minoda, Y., M. Aihara, A. Sakawa, S. Fukuoka, K. Hayakawa, M. Tomita, N. Umeda, and K. Ohzono. 2009. 'Comparison between highly cross-linked and conventional polyethylene in total knee arthroplasty', *Knee*, 16: 348-51.
- Muratoglu, Orhun K, Brian R Burroughs, Charles R Bragdon, Steven Christensen, Andrew Lozynsky, and William H Harris. 2004. 'Knee simulator wear of polyethylene tibias articulating against explanted rough femoral components', *Clinical orthopaedics and related research*, 428: 108-13.
- Muratoglu, Orhun K., Jeff Ruberti, Suzi Melotti, Stephen H. Spiegelberg, Evan S. Greenbaum, and William H. Harris. 2003. 'Optical analysis of surface changes on early retrievals of highly cross-linked and conventional polyethylene tibial inserts', *The Journal of arthroplasty*, 18: 42-47.
- "National Joint Registry For England, Wales, Northern Ireland and Isle of Man." In. 2019. *15th Annual Report*.
- Paxton, E. W., M. C. Inacio, S. Kurtz, R. Love, G. Cafri, and R. S. Namba. 2015. 'Is there a difference in total knee arthroplasty risk of revision in highly crosslinked versus conventional polyethylene?', *Clin Orthop Relat Res*, 473: 999-1008.
- Petersen, T.L., and G.A. Engh. 1988. 'Radiographic Assessment of Knee Alignment After Total Knee Arthroplasty', *Journal of Arthroplasty*: 67-72.
- "Register of the Orthopaedic Prosthetic Implants." In. 2017. Bologna: Instituto Ortopedico Rizzoli.
- Ruggiero, Alessandro, Massimiliano Merola, and Saverio Affatato. 2017. 'On the biotribology of total knee replacement: a new roughness measurements protocol on in vivo condyles considering the dynamic loading from musculoskeletal multibody model', *Measurement*, 112: 22-28.
- Saikko, Vesa, Vesa Vuorinen, and Hannu Revitzer. 2016. 'Effect of CoCr Counterface Roughness on the Wear of UHMWPE in the Noncyclic RandomPOD Simulation', *Journal of Tribology*, 139.
- Sakellariou, V. I., P. Sculco, L. Poultsides, T. Wright, and T. P. Sculco. 2013. 'Highly cross-linked polyethylene may not have an advantage in total knee arthroplasty', *HSS J*, 9: 264-9.
- Sato, T., Y. Nakashima, M. Akiyama, T. Yamamoto, T. Mawatari, T. Itokawa, M. Ohishi, G. Motomura, M. Hirata, and Y. Iwamoto. 2012. 'Wear resistant performance of highly

- cross-linked and annealed ultra-high molecular weight polyethylene against ceramic heads in total hip arthroplasty', *J Orthop Res*, 30: 2031-7.
- Scholes, Susan C, Emma Kennard, Rajkumar Gangadharan, David Weir, Jim Holland, David Deehan, and Thomas J Joyce. 2013. 'Topographical analysis of the femoral components of ex vivo total knee replacements', *Journal of Materials Science: Materials in Medicine*, 24: 547-54.
- Sharma, Ankur. 2018. 'Evaluation of Knee Kinematics in Single Radius versus Multi-Radii Total Knee Arthroplasty in India Population : A Randomized Control Trial', *Open Access Journal of Biomedical Engineering and Biosciences*, 1.
- Sheehy, L., D. Felson, Y. Zhang, J. Niu, Y. M. Lam, N. Segal, J. Lynch, and T. D. Cooke. 2011. 'Does measurement of the anatomic axis consistently predict hip-knee-ankle angle (HKA) for knee alignment studies in osteoarthritis? Analysis of long limb radiographs from the multicenter osteoarthritis (MOST) study', *Osteoarthritis Cartilage*, 19: 58-64.
- Sisko, Z. W., M. G. Teeter, B. A. Lanting, J. L. Howard, R. W. McCalden, D. D. Naudie, S. J. MacDonald, and E. M. Vasarhelyi. 2017. 'Current Total Knee Designs: Does Baseplate Roughness or Locking Mechanism Design Affect Polyethylene Backside Wear?', *Clin Orthop Relat Res*, 475: 2970-80.
- Stavrakis, A., L. Weitzler, T. Wright, and D. E. Padgett. 2018. 'Less Midterm Damage and Oxidation Are Seen in Retrieved Highly Crosslinked Ultrahigh-Molecular-Weight Polyethylene Tibial Inserts than in Direct Compression Molded Polyethylene Inserts', *HSS J*, 14: 159-65.
- Stoddard, J. E., D. J. Deehan, A. M. Bull, A. W. McCaskie, and A. A. Amis. 2013. 'The kinematics and stability of single-radius versus multi-radius femoral components related to mid-range instability after TKA', *J Orthop Res*, 31: 53-8.
- Stoner, K. E., N. A. Nassif, T. M. Wright, and D. E. Padgett. 2013. 'Laser scanning as a useful tool in implant retrieval analysis: a demonstration using rotating platform and fixed bearing tibial inserts', *J Arthroplasty*, 28: 152-6.
- Willie, B. M., L. J. Foot, M. W. Prall, and R. D. Bloebaum. 2008a. 'Examining the influence of short-term implantation on oxidative degradation in retrieved highly crosslinked polyethylene tibial components', *J Biomed Mater Res B Appl Biomater*, 85: 385-97.
- . 2008b. 'Surface damage analysis of retrieved highly crosslinked polyethylene tibial components after short-term implantation', *J Biomed Mater Res B Appl Biomater*, 85: 114-24.

## Appendix A

Study done to validate the accuracy of laser scanner

An intentional scratch was made on the nonbearing surface of a PE insert and scanned using the laser scanner and compared with a reference insert in the GOM software. The average deviation of the scratch was calculated to be  $-0.062 \pm 0.010$  mm (figure A.1 (i)). The depth of the scratch was also measured using a two-dimensional (2D) contacting profilometer (Mitutoyo Surftest SJ-210). The average depth of the scratch was found to be  $-0.071 \pm 0.027$  mm. The depth profile obtained at two different positions of the scratch is shown in figure A.1 (ii, iii).

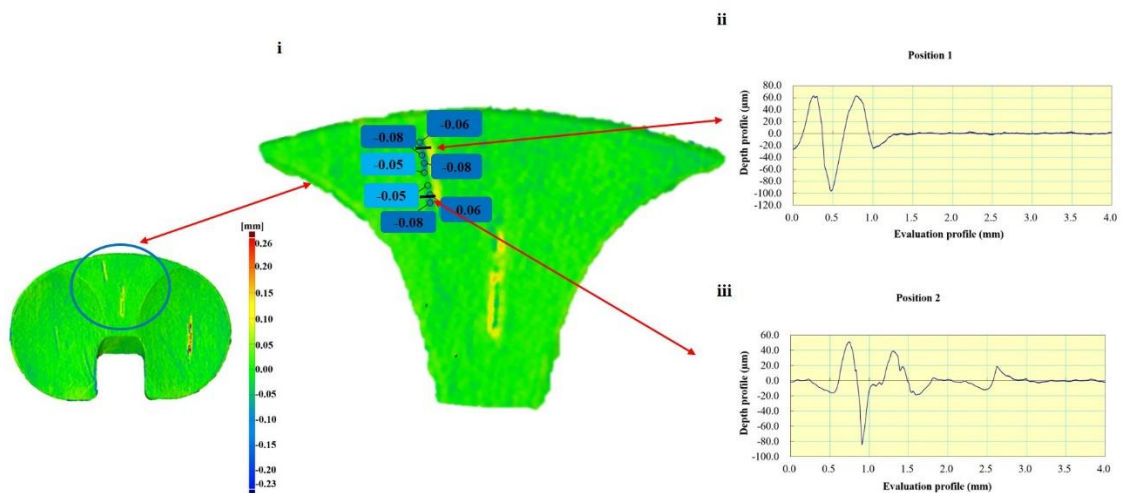


**Figure A.1** (i) Deviation values shown at different positions of an intentional scratch on the non-bearing region of the component; depth profile obtained at (ii) position 1 (iii) position 2 of a scratch

## Acknowledgement

The authors acknowledge the support of William Leech Charity towards the current project.